

## The Late Cretaceous East Sikhote-Alin Volcanic Belt: Transition from Subduction to Sliding of Lithospheric Plates (Structure-Geological, Petrological, and Isotope-Geochemical Aspects)

A.Yu. Martynov , V.V. Golozubov, Yu.A. Martynov, S.A. Kasatkin

Far East Geological Institute, Far Eastern Branch of the Russian Academy of Sciences,  
pr. 100-letiya Vladivostoka 159, Vladivostok, 690022, Russia

Received 3 July 2017; received in revised form 1 November 2018; accepted 8 November 2018

**Abstract**—The East Sikhote-Alin volcanic belt extending for ~1500 km is commonly considered a single tectonomagmatic structure formed during the Late Cretaceous subduction and the Cenozoic oceanic-slab breakup and active asthenospheric diapirism under transform plate sliding. Based on analysis of the published geological information and the new data on the age and trace-element and isotope compositions of the igneous rocks of the Late Cretaceous Bol’ba Formation, it is shown that the initial stages of volcanism in the southern and northern Sikhote-Alin took place in different geodynamic settings. In contrast to the coeval suprasubduction volcanics of the southern sector (Primorye), the volcanic section of the Bol’ba Formation is dominated by magnesian ( $Mg\# = 26–40$ ) adakites ( $La/Yb = 19–34$ ) and high-Nb basalts. This igneous rock association and the lead ( $\Delta 8/4Pb = 30–46$ ) and neodymium ( $0.51279–0.51281$ ) isotope ratios of the studied rocks suggest the influence of the “hot” oceanic asthenosphere on magma genesis. The earlier slab breakup north of  $48–49^\circ N$  was due to the oblique convergence of oceanic and continental lithospheric plates in the Late Cretaceous, accompanied by sinistral shears. The results obtained indicate that the lateral zonation of the eastern Sikhote-Alin is due to different geodynamic settings of formation of its northern and southern sectors rather than variations in its basement composition. In theoretical aspect, the performed research is important for the correct reconstruction of the geologic events in zones of convergence of oceanic and continental plates. It is necessary to take into account not only the general direction of the convergence but also the configuration of the plate boundary.

**Keywords:** lateral nonuniformity, northern sector, Cretaceous volcanism, adakites, high-Nb basalts, geodynamics, eastern Sikhote-Alin

### INTRODUCTION

The East Sikhote-Alin volcanic belt of Late Cretaceous and Cenozoic volcanics is traceable in the NE direction along the coast of the Sea of Japan and the Tatar Strait. It forms a 20–30 to 100 km thick band stretching for ~1500 km from Cape Ostrovnoi in the south ( $\sim 43^\circ N$ ) to the mouth of the Amur River (Fig. 1). Today it is considered to be a single tectonomagmatic structure resulted from the Late Cretaceous subduction processes and the Cenozoic breakup of an oceanic slab and intrusion of the oceanic asthenosphere into the suprasubductional mantle (Martynov et al., 2017). This conclusion was drawn based on results of a comprehensive research into volcanism in the southern sector of the belt (Primorye). The geology and petrology of the northern sector have been poorly studied. The present paper is an attempt to fill this gap by geological and isotope-geochemical studies of the volcanics of the Late Cretaceous Bol’ba Formation.

### GEOLOGICAL OUTLINE

The East Sikhote-Alin volcanic belt (ESAVB), first recognized by N.S. Shatskii in 1957, includes Late Cretaceous–Pliocene volcanic and associated intrusive rocks (Fig. 1). It was earlier considered to be the result of subduction of the Kula and Pacific oceanic plates beneath the Eurasian continent (150–60 Ma) (Zonenshain et al., 1990). Recent geological and petrological data show that only the Late Cretaceous volcanics can be referred to as typical subductional, whereas the Cenozoic igneous rocks of intermediate and mafic compositions resulted from the breakup of a Late Cretaceous oceanic slab and the intrusion of the oceanic asthenosphere into the subcontinental lithosphere (Martynov et al., 2017).

Many researchers, beginning from Izokh (1966), assumed a lateral zonation of the ESAVB, caused by E–W striking faults dividing the structure into a number of blocks with different types of magmatism and metallogeny. This issue was not considered in detail, but there are distinct signs of such a zonation:

(1) Different thicknesses of the Earth’s crust, from ~40 km in the south to ~25–30 km in the north (Lishnevskii, 1969; Argentov et al., 1976).

 Corresponding author.

E-mail address: amartynov@fegi.ru (A.Yu. Martynov)

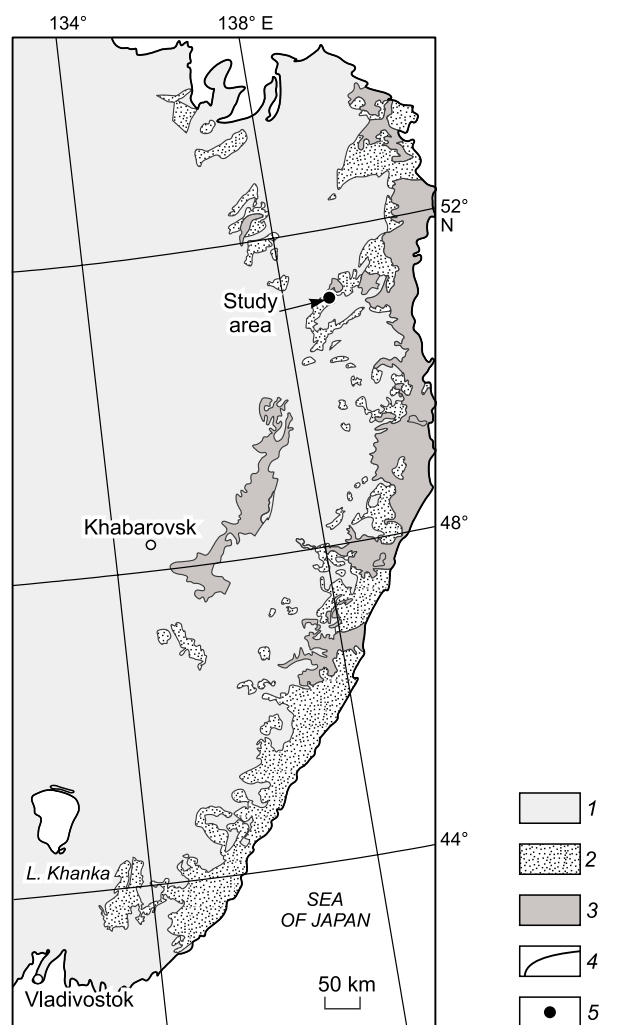


**Fig. 1.** Schematic geological map of the East Sikhote-Alin volcanic belt, after Krasnyi and Peng Yunbiao (1998), modified. 1, pre-Late Cretaceous deposits; 2, 3, volcanics of the ESAVB: 2, Late Cretaceous, 3, Cenozoic; 4, major faults; 5, study area.

(2) Different compositions of the basement. In the south it is formed by the terrigenous rocks of the Kema terrane (Khanchuk, 1993) uniting the island-arc deposits regarded earlier as the Aptian–Turonian East Sikhote-Alin (Parfenov, 1984; Natal'in and Borukaev, 1991) or the Samarga (Simanenko, 1986, 1990) island arc. In the north, the basement is the Lower Amur accretionary-prism terrane composed of sheets of basalts or, sometimes, gabbroids of MORB composition, Jurassic siliceous-carbonate rocks, and Early Cretaceous (to Aptian) flints.

(3) Different structures and compositions of the Late Cretaceous and Cenozoic volcanic strata. In the southern sector, the Late Cretaceous continental volcanosedimentary deposits are: (a) tuff conglomerates, tuffstones, and felsic tuffs of the Petrozuevka Formation (Late Albian(?)-Cenomanian); (b) andesites, basaltic andesites, and their tuffs of the Sinancha Formation (Cenomanian); (c) ignimbrites, rhyolite tuffs, and, seldom, tuffstones and tuffaceous siltstones of the Pri-

morye Group (Turonian–Campanian); (d) andesites, basaltic andesites, and their tuffs of the Samarga Formation (Maastriichtian) (Mikhailov, 1989). According to the geochemical features, the Late Cretaceous volcanics are suprasubductional rocks formed on an active margin of the Andean type (Simanenko and Khanchuk, 2003; Martynov et al., 2007). Cenozoic felsic and mafic volcanics are of limited occurrence in the south of the belt.

North of 49° N, Late Cretaceous volcanic rocks are mapped in: (a) the folded basement (tuff, andesite lava, and basalt lava horizons in the section of marine terrigenous sediments, which are united into the Cenomanian Utitsa Formation) (Kudymov et al., 2015) and (b) the postfolded sheet formed by younger Campanian–Maastriichtian(?) surficial igneous rocks. The latter include andesite and basaltic-andesite lavas of the Bol'ba Formation (Sidorenko, 1968). Oligocene–Miocene basalts are the most widespread among the Cenozoic volcanics; they compose a large area along the coast of the Tatar Strait, from De Kastri Bay to the mouth of the Tumnin River.

(4) The southern and northern sectors of the ESAVB differ in paleomagnetic characteristics (Didenko et al., 2017). The surface of the bottom of the magnetic layer (isotherm 578 °C, the Curie point of magnetite) within the eastern Sikhote-Alin has a cellular pattern. Its minimum depths (16–20 km), however, are established in the north of the belt, which indicates heating of the lower crust and the upper mantle.

(5) The two ESAVB sectors show different metallogenic signatures: There is predominantly Sn and Pb–Zn mineralization in the south and Au–Ag mineralization in the north.

Additional research can clarify whether or not the above differences are due to the specific structure of the basement and the specific geodynamic settings of its formation in the Late Cretaceous or Cenozoic. Here we consider these issues, using the new field and isotope-geochemical data on the mafic and intermediate volcanics of the Campanian Bol'ba complex in the northern Sikhote-Alin.

## SAMPLES AND METHODS

For petrographic and analytical studies we used a representative collection of 33 samples with minimum visible signs of metasomatism (Table 1).

The samples were prepared on Russian and German Fritsch equipment for treatment of geologic samples, with their quality and purity monitoring. The transparent thin sections of the samples were described using a modern ERGAVAL CARL ZEISS JENA (Germany) polarization microscope at the Far East Geological Institute, Vladivostok.

The contents of rock-forming oxides were determined at the Analytical Center of the Far East Geological Institute, Vladivostok. The contents of major elements were determined by gravimetry ( $\text{SiO}_2$ ) and atomic-emission spectrometry with inductively coupled plasma (ICP-AES) ( $\text{TiO}_2$ ,  $\text{Al}_2\text{O}_3$ ,  $\text{FeO}^*$ ,  $\text{CaO}$ ,  $\text{MgO}$ ,  $\text{MnO}$ ,  $\text{K}_2\text{O}$ ,  $\text{Na}_2\text{O}$ , and  $\text{P}_2\text{O}_5$ ), us-

**Table 1.** Coordinates of the sampling localities in the basin of the Shelekhov Brook

Sample	Type of rock (field and microscopic observations)	Coordinates, N, E
Ya10	Andesites	50°57' 04.2" 138°29'59.3"
Ya11		
Ya12		
Ya13	Granodiorite	50°53' 26.1" 138°33'44.1"
Ya13(a)	Basaltic andesite	
Ya13(b)	Andesite	
Ya13(c)	Dacite	
Ya13(d)	Andesite	
Ya14(a)	Granite	50°53' 27.3" 138°33'39.3"
Ya14(b)	Granite	
Ya15	Andesite	50°53' 31.8" 138°33'29.3"
Ya16	Granodiorite	50°53' 36.3" 138°33'23.6"
Ya16(a)	Gabbro	
Ya16(b)	Gabbro-diorite	
Ya16(c)	Andesite	
Ya17	Basalt	50°53' 41.3" 138°33'17.8"
Ya18	Basalt	50°53' 59.3" 138°33'03.0"
Ya19	Diorite	50°53' 50.9" 138°33'24.6"
Ya20	Diorite	50°53' 47.1" 138°33'30.1"
Ya20(a)		
Ya21	Basaltic andesite	50°54' 05.0" 138°32'53.5"
Ya22	Basalt	50°54' 08.8" 138°32'53.0"
Ya23	Basaltic andesite	50°54' 08.8" 138°32'53.0"
Ya24	Andesite	50°54' 19.5" 138°32'43.1"
Ya25	Andesite	50°54' 49.7" 138°32'15.8"
Ya26 Ya26(1)	Andesite	50°54' 49.7" 138°32'15.8"
Ya27	Basalts	
Ya27(1)	Basalts	50°55' 25.7" 138°31'00.5"
Ya27(2)	Basalts	50°55' 27.4" 138°30'57.6"
Ya28	Basalts	50°55'32.8" 138°30'58.1"
Ya29	Basalts	50°55'36.1" 138°30'57.9"
Ya30	Basalts	50°55'17.3" 138°31'19.1"

ing an ICAP 6500 Duo (Thermo Electron Corporation, USA) spectrometer. Cadmium solution (10 ppm) was added as an internal standard (analysts V.N. Kaminskaya, M.G. Blokhin, and G.I. Gorbach). The samples were decomposed in a mixture of HF, HNO<sub>3</sub>, and HClO<sub>4</sub> (superpure, Merck) (2.5:1:0.5). Calibration solutions were prepared from the DVA, DVB, DVD, DVR, and SA-1 standard samples (Russia) by open decomposition. Trace elements were determined by ICP-MS on an Agilent 7500 quadrupole mass spectrometer (Agilent Technologies, USA), using <sup>115</sup>In (10 ppb) as an internal standard. The certified CLMS-1, CLMS-2, CLMS-3, and CLMS-4 multielement solutions (USA) were used for calibration, and the geologic JB-2 and JB-3 basalt and JA-2 andesite samples (Japan) were applied as standards.

The isotope parameters (<sup>143</sup>Nd/<sup>144</sup>Nd, <sup>208</sup>Pb/<sup>204</sup>Pb, <sup>207</sup>Pb/<sup>204</sup>Pb, and <sup>206</sup>Pb/<sup>204</sup>Pb) of the representative samples were determined at the Institute of Precambrian Geology and Geochronology, St. Petersburg. The preparation of the

samples for Nd isotope analyses included their chemical decomposition and the following ion exchange chromatographic separation of elements by the technique described in detail by Savatenkov et al. (2004). The Nd isotope composition was measured on a Triton multicollector solid-phase mass spectrometer. The reproducibility of the results was controlled by analysis of the La Jolla and SRM-987 standards.

Chemical separation of Pb from rocks was made by a standard technique. The Pb isotope composition was measured on a Finnigan MAT-261 multicollector mass spectrometer in the regime of simultaneous recording of the ionic currents of different elements. The measurements were carried out in a single-tape regime on rhenium evaporators, using a silicate emitter in mixture with H<sub>3</sub>PO<sub>4</sub>. The total laboratory contamination with Pb was no higher than 0.1 ng. The Pb isotope ratios were corrected for fractionation by the double isotope dilution method, using a <sup>204</sup>Pb/<sup>207</sup>Pb tracer (Mel'nikov, 2005).

K–Ar dating was performed for biotite grains (selected manually under a binocular) at the Analytical Center of the Far East Geological Institute, Vladivostok. The contents of Ar isotopes were measured by CF–GC–IRMS in a steady helium flow in the Laboratory of Stable Isotopes of this institute (Ignatiev et al., 2009; Budnitskiy et al., 2013). According to the reported technique, argon is separated from the sample by CO<sub>2</sub> laser and passes in a helium flow through a chromatographic column, where it is separated from other impurity gases. Then, argon in a helium flow gets through a splitter into the ion source of a Finnigan MAT-253 mass spectrometer. The signals of isotopes <sup>36</sup>Ar, <sup>38</sup>Ar, and <sup>40</sup>Ar are measured in the dynamic regime on three collectors at once (Budnitskiy et al., 2013). The error of determination of radiogenic argon was within 1% at the 2σ confidence level. The portion of air argon was 5–10%. The content of K in the samples was measured by flame photometry, with the measurement error of 2%. The error of the calculated age was 3% and was controlled by the convergence of the results of repeated analyses of the samples and by the reproducibility of the analytical results for the standard samples. There were, on average, four measurements for each sample. The age was calculated using the constants λ<sub>e</sub> = 0.581 × 10<sup>-10</sup> yr<sup>-1</sup> and λ<sub>β</sub> = 4.962 × 10<sup>-10</sup> yr<sup>-1</sup> (Steiger and Jäger, 1977).

## RESULTS

### Geologic structure

The Bol'ba Formation was first recognized and described by B.Ya. Abramson on the right bank of the Amur River near the Bol'ba cliff (between the Tsimmermanovka and Sofiiskoe Villages) in 1956 (Sidorenko, 1968). He regarded it as alternation of terrestrial volcanic and volcanosedimentary rocks overlying, with an angular unconformity, the Middle–Late Albian Udoma Formation. In the stratotype

section, a 20.6 m thick member of tuff conglomerates alternating with interbeds of tuffstones, andesite tuffs, and tuffites is mapped in the bottom of the Bol’ba Formation. Upsection, there are denuded andesite flows separated by numerous horizons of volcanosedimentary rocks (tuff conglomerates and tuffstones). The total thickness of the formation is estimated at 400 m (Sidorenko, 1968).

Among the numerous plant remains collected by B.Ya. Abramson in 1956, M.O. Borsuk identified a complex of plants typical of the Upper Cretaceous high horizons (Sidorenko,

1968). The age of the plants is confirmed by K–Ar isotope dates obtained by Sukhov (1967) for the formation rocks, 70–85 Ma. The Bol’ba Formation is much younger than the Sinancha Formation (Cenomanian) in the Primorye segment of the ESAVB. Thus, these formations are not age analogs, as sometimes assumed (Freidin and Lifshits, 1957). The Bol’ba Formation is either not an age analog of the Samarga Formation dated at the Maastrichtian (Mikhailov, 1989).

We studied an exposure of the Bol’ba Formation in the basin of the middle stream of the Shelekhov Brook (Fig. 2).

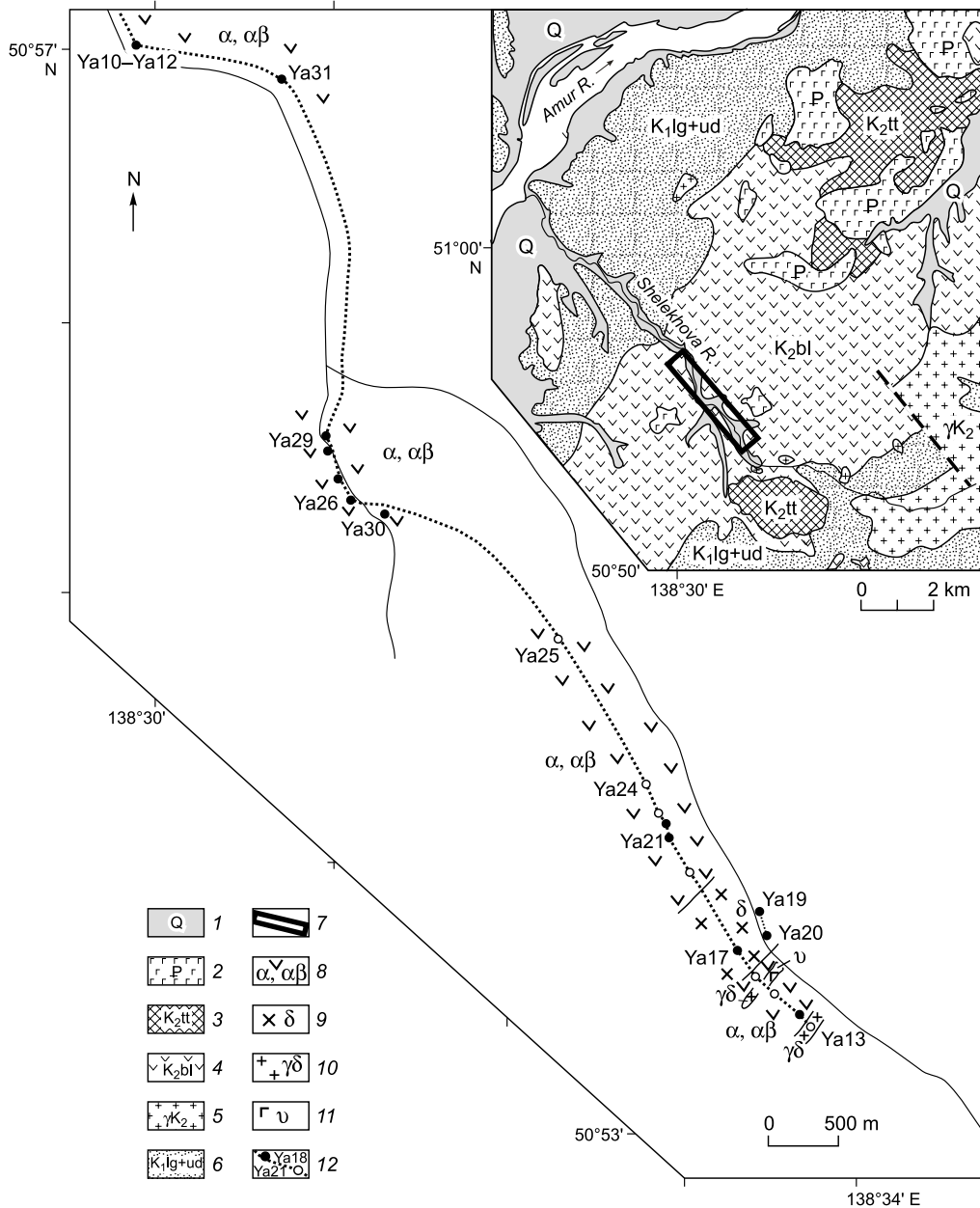


**Fig. 2.** Location of the study area. Inset at the upper right is a fragment of a geological map of the study area, after Freidin and Lifshits (1957), modified. 1, Quaternary alluvial sediments; 2, Paleogene basalts; 3, 4, Late Cretaceous volcanic complexes: 3, felsic volcanic rocks of the Tatar Formation, 4, andesites and basaltic andesites of the Bol’ba Formation; 5, Late Cretaceous granites; 6, terrigenous deposits of the Middle–Upper Albian Largasu and Udoma Formations; 7, study area; 8–12, legend to a route map: 8–11, outcrops of rocks of the Bol’ba Formation: andesites and basaltic andesites (8), granodiorites (10), and gabbro (11); 12, route line, observation points and their numbers. Dark circles mark the localities of sampling of bedrocks, and light circles, sampling in block taluses.

Northwest of it, in the lower stream of the brook, the rocks of the folded basement expose. The basement is composed of intensely dislocated Lower Cretaceous marine sedimentary, mostly argillaceous deposits earlier ascribed to the Largasu Formation. Southeast of the study area, in the upper stream of the brook, the folded basement includes terrigenous rocks (sandstones, siltstones, and, more seldom, conglomerates) earlier ascribed to the Middle–Late Albian Largasu and Udoma Formations (Markevich et al., 2000). The marginal part of a large granite massif exposes in the source of the brook. The zone of contact metamorphism of the massif includes both sedimentary rocks and the volcanics of the Bol’ba Formation.

Samples for study were taken from the coastal exposures and block taluses on the left bank of the brook (Fig. 2), where rocks are mostly of lava and subvolcanic facies. The lava facies are composed of dark gray massive, predominantly cryptocrystalline andesites and basaltic andesites, often with plagioclase phenocrysts. In the upper stream of the Shelekhov Brook, we found outcrops of obviously subvolcanic rocks of different compositions. Among them there is a large (250 × 700 m) outcrop of massive fine-grained gabbro, gabbro-diorites (samples Ya16(a), Ya16(b), Ya17, Ya19, and Ya20), and pinkish-gray medium-grained granodiorites (samples Ya13 and Ya16). We did not observe direct contacts between these rocks and the host flood volca-

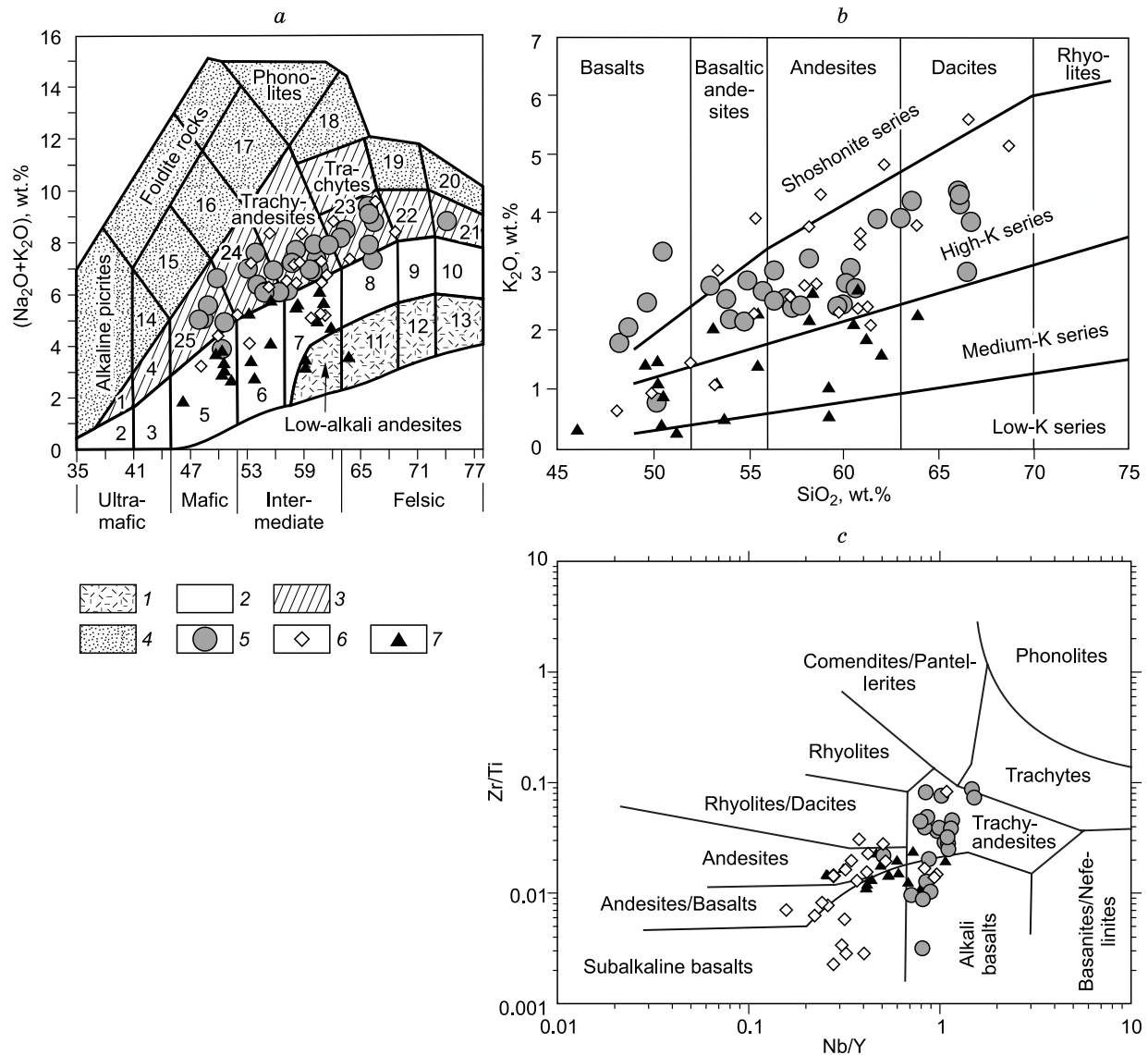


**Fig. 3.** Classification diagrams: *a*,  $(\text{Na}_2\text{O} + \text{K}_2\text{O})$ – $\text{SiO}_2$  (Bogatikov et al., 2009), *b*,  $\text{K}_2\text{O}$ – $\text{SiO}_2$ , *c*,  $\text{Zr/Ti}$ – $\text{Nb/Y}$  (Winchester and Floyd, 1977). *a*: 1, medium-alkali picrites, 2, picrites, 3, basalts, 4, medium-alkali picrite basalts, 5, basalts, 6, basaltic andesites, 7, andesites, 8, dacites, 9, rhyodacites, 10, rhyolites, 11, low-alkali dacites, 12, low-alkali rhyodacites, 13, low-alkali rhyolites, 14, alkali picrite basalts, 15, alkali basalts, 16, phonotephrites, 17, tephriphonolites, 18, alkali trachytes, 19, alkali rhyodacites, 20, alkali rhyolites, 21, trachyrhyolites, 22, trachyrhyodacites, 23, trachydacites, 24, basaltic trachyandesites, 25, trachybasalts. 1–4, rocks: 1, low-alkali, 2, normal-alkaline, 3, medium-alkali, 4, alkaline, 5, Bol’ba Formation; 6, Samarga Formation (Martynov et al., 2007); 7, Sinancha Formation (Simanenkov and Khanchuk, 2003).

**Table 2.** Contents of major oxides (wt.%) and trace elements (ppm) in representative rock samples from the Bol'ba complex

Element	Ya10	Ya20	Ya16	Ya27(2)	Ya20(a)	Ya26	Ya13	Ya27(1)	Ya-29	Ya-17	Ya-16(b)	Ya-16(a)	Ya-30	Ya-29	Ya-12	Ya-11
SiO <sub>2</sub>	60.45	60.04	66.10	57.40	59.75	56.45	66.00	66.48	57.06	53.11	54.88	49.80	48.36	57.06	60.70	60.22
TiO <sub>2</sub>	0.90	0.89	0.66	1.17	0.89	1.25	0.48	0.57	1.21	1.57	1.21	1.72	1.83	1.21	0.89	0.94
Al <sub>2</sub> O <sub>3</sub>	16.57	16.29	16.07	15.57	16.15	15.97	15.78	16.70	15.89	16.62	16.11	17.01	16.51	15.89	16.55	16.86
FeO*	5.23	5.33	3.16	6.29	5.54	6.66	2.79	3.71	6.64	8.10	7.50	9.12	9.17	6.64	5.02	5.33
MnO	0.09	0.10	0.08	0.09	0.10	0.12	0.06	0.06	0.12	0.16	0.13	0.16	0.14	0.12	0.09	0.09
MgO	2.36	3.43	1.30	4.21	3.29	3.72	1.11	0.76	3.48	4.16	5.47	4.89	6.16	3.48	2.57	2.71
CaO	4.17	4.71	2.65	5.34	5.28	6.21	1.78	3.15	6.53	7.02	6.94	7.62	8.42	6.53	4.36	2.84
Na <sub>2</sub> O	4.28	4.41	4.76	3.74	4.52	3.04	5.00	4.31	3.57	4.20	3.91	4.13	3.25	3.57	4.24	5.10
K <sub>2</sub> O	3.07	2.45	4.33	2.39	2.42	3.03	4.40	3.01	2.56	2.77	2.16	2.48	1.79	2.56	2.73	2.81
P <sub>2</sub> O <sub>5</sub>	0.38	0.39	0.23	0.59	0.39	0.61	0.19	0.19	0.61	0.69	0.38	0.73	0.68	0.61	0.38	0.40
LOI	1.83	1.25	0.38	2.22	1.10	1.96	2.05	0.81	1.52	0.59	0.43	1.28	2.19	1.52	1.60	2.01
Total	100.31	100.24	100.28	100.19	100.28	100.20	100.19	1000.36	100.34	100.31	100.22	100.28	100.23	100.98	100.09	100.34
Cs	0.84	3.11	2.17	0.71	1.24	0.93	2.36	3.79	0.74	2.12	3.83	1.76	0.48	0.74	1.21	1.07
Rb	85.75	55.67	103.81	47.75	54.47	56.90	112.79	78.99	56.06	57.19	50.56	54.98	29.75	56.06	72.94	72.64
Ba	747	604	697	558	599	856	595	602	638	672	412	611	416	638	647	618
Th	10.06	8.09	13.71	6.08	7.53	6.88	14.00	12.89	6.81	6.18	5.85	4.17	3.29	6.81	10.66	9.60
U	2.76	1.72	3.18	1.87	1.64	2.03	3.57	3.62	1.96	1.50	1.58	1.03	0.79	1.96	2.92	2.58
Nb	15.01	13.97	23.04	18.15	13.86	18.66	18.91	9.09	18.81	15.85	12.82	16.42	19.40	18.81	15.15	15.02
Ta	1.32	1.16	1.94	1.35	1.14	1.37	1.77	1.04	1.41	1.18	0.99	1.11	1.38	1.41	1.31	1.30
La	38.85	37.29	43.24	40.82	37.44	41.80	41.93	30.54	42.98	39.98	27.84	39.45	33.54	42.98	37.84	36.58
Ce	71.65	67.94	77.36	81.40	68.44	83.45	74.34	57.49	85.31	84.63	56.84	83.78	74.78	85.31	71.89	70.61
Pb	14.82	10.26	14.53	10.82	9.56	9.72	14.01	15.90	9.91	9.18	6.80	8.12	5.82	9.91	10.64	9.99
Pr	8.14	7.59	8.32	9.52	7.60	9.67	7.91	6.09	9.84	10.22	6.61	10.26	9.40	9.84	7.92	7.95
Nd	30.65	28.71	28.95	37.17	28.08	37.40	27.27	22.08	37.93	40.38	25.68	40.13	38.72	37.93	30.01	30.12
Sm	5.47	5.20	4.78	6.82	4.85	6.70	4.53	3.75	6.84	7.71	5.11	7.67	7.58	6.84	5.42	5.48
Zr	155	42	33	141	38	168	79	56	170	30	70	92	115	170	149	142
Hf	4.91	1.40	1.50	4.56	1.24	5.08	3.00	2.56	5.29	1.24	2.41	3.02	4.05	5.00	4.95	4.60
Eu	1.42	1.48	1.13	1.65	1.38	1.75	1.05	1.07	1.81	2.00	1.38	1.96	2.06	1.81	1.38	1.36
Gd	5.35	5.08	4.60	6.15	4.78	6.29	4.25	3.44	6.35	7.06	5.04	6.99	7.26	6.35	5.18	5.19
Tb	0.68	0.67	0.60	0.77	0.59	0.80	0.57	0.43	0.81	0.92	0.73	0.94	0.99	0.81	0.66	0.67
Dy	3.47	3.28	3.22	3.68	3.07	3.89	2.94	2.01	3.96	4.56	4.02	4.70	5.03	3.96	3.39	3.48
Y	14.91	15.71	15.28	15.54	14.16	15.98	14.55	8.56	16.53	19.69	18.07	20.36	21.75	16.35	14.42	14.68
Ho	0.67	0.64	0.63	0.70	0.58	0.70	0.59	0.37	0.73	0.85	0.80	0.87	0.99	0.73	0.65	0.65
Er	1.90	1.75	1.84	1.88	1.67	1.99	1.74	1.05	2.04	2.31	2.22	2.50	2.68	2.04	1.83	1.92
Tm	0.25	0.22	0.25	0.24	0.21	0.25	0.26	0.14	0.25	0.31	0.32	0.31	0.34	0.25	0.25	0.25
Yb	1.65	1.41	1.66	1.46	1.31	1.64	1.66	0.90	1.60	1.88	1.96	2.09	2.08	1.60	1.62	1.63
Lu	0.25	0.21	0.24	0.21	0.18	0.24	0.25	0.14	0.23	0.29	0.28	0.30	0.30	0.23	0.24	0.23
Mg#	31	39	29	40	37	36	28	17	34	34	42	35	40	34	34	34
La/Yb	24	26	26	28	29	26	25	34	27	21	14	19	16	27	23	22
Sm/Yb	3.31	3.70	2.87	4.67	3.70	4.08	2.72	4.10	4.27	4.10	2.60	3.66	3.64	4.27	3.34	3.36
<sup>143</sup> Nd/ <sup>144</sup> Nd	–	–	–	–	–	–	–	–	–	0.51279	0.51281	0.51280	–	–	–	–
<sup>206</sup> Pb/ <sup>204</sup> Pb	–	–	–	–	–	–	–	–	–	18.6343	18.7712	18.6350	–	–	–	–
<sup>207</sup> Pb/ <sup>204</sup> Pb	–	–	–	–	–	–	–	–	–	15.5612	15.5782	15.6000	–	–	–	–
<sup>208</sup> Pb/ <sup>204</sup> Pb	–	–	–	–	–	–	–	–	–	38.4906	38.6238	38.6240	–	–	–	–

Note. FeO\*, total iron as FeO; Mg # = MgO/(MgO + FeO\*), wt.%; LOI, loss on ignition.

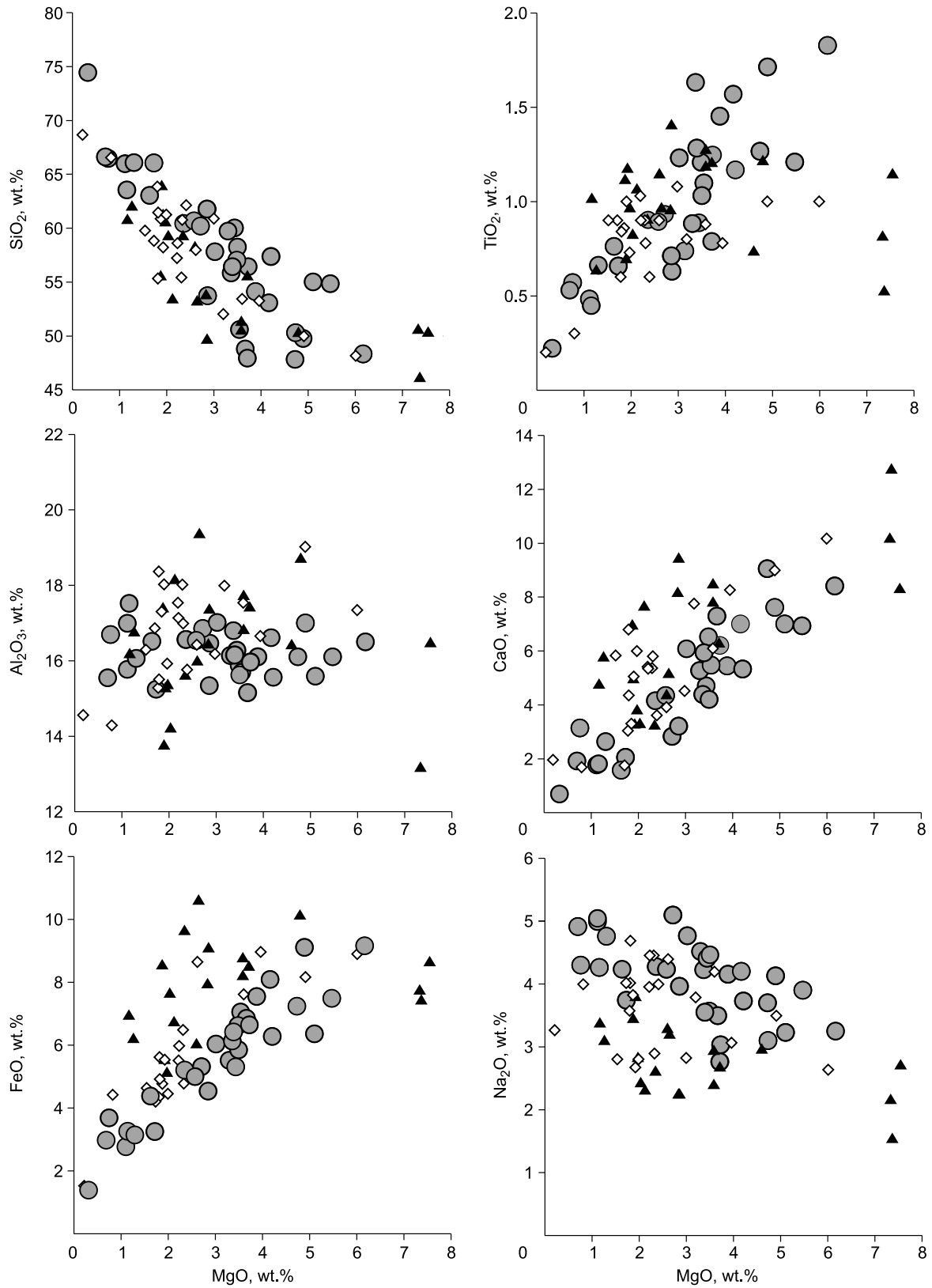


**Fig. 4.** Rock-forming elements vs. MgO. Designations follow Fig. 3.

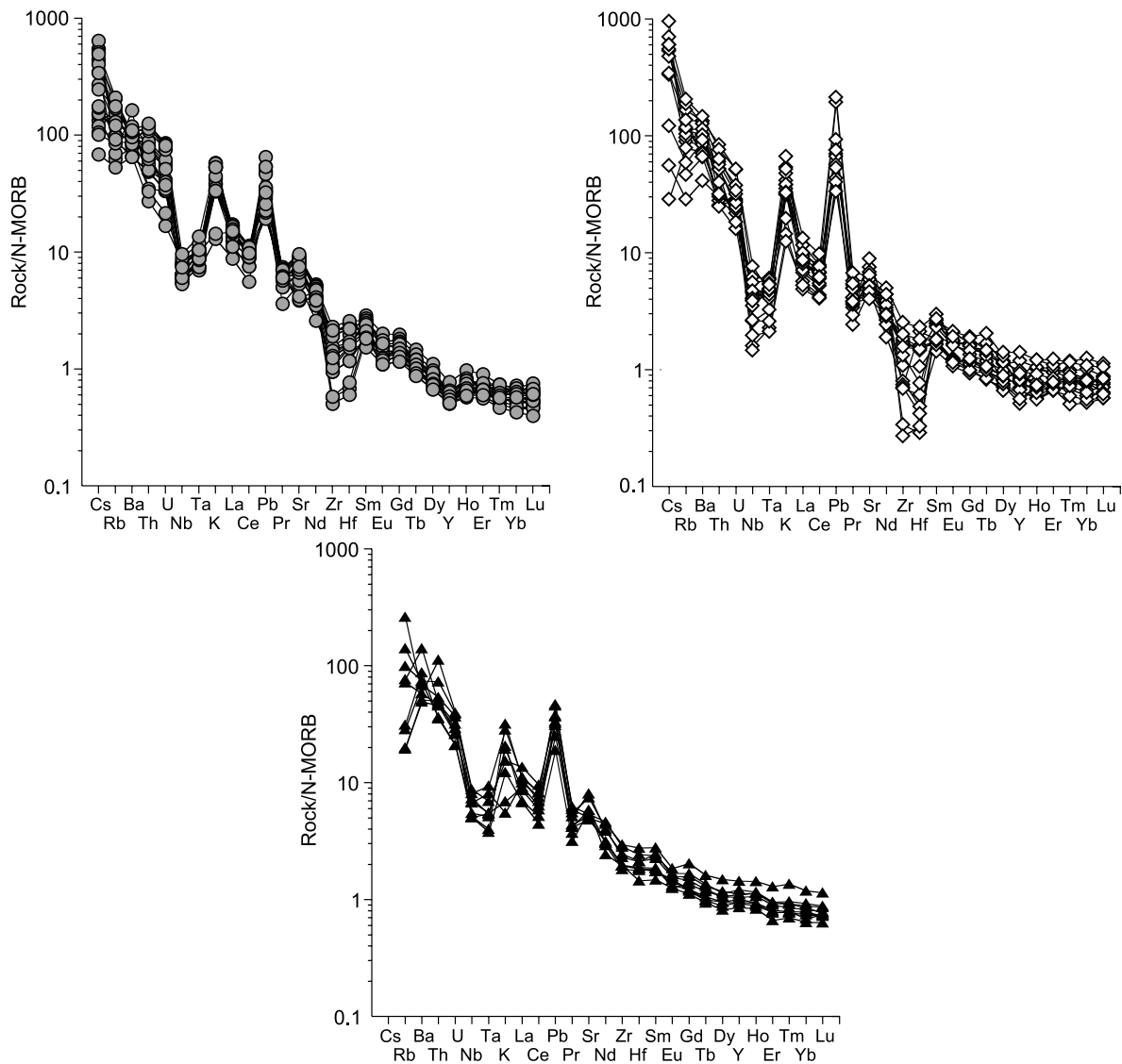


Fig. 5. N-MORB-normalized (Sun and McDonough, 1989) trace-element patterns. Designations follow Fig. 3.

tics, but, as shown below, the main geochemical features of the rocks testify to their belonging to the Bol'ba Formation. This is confirmed by results of K–Ar dating of biotite grains from subvolcanic gabbro (sample Ya16a) from the upper stream of the Shelekhov Brook. By mineral composition it can be assigned to the plagioclase–two-pyroxene–biotite type with minimum petrographic and petrochemical signs of secondary alterations. The obtained date ( $74.5 \pm 5.1$ , Campanian–Maastrichtian) agrees with the earlier paleobotanic and K–Ar dates for the stratiform rocks of the Bol'ba Formation (Sukhov, 1967).

### Petrography

The basalts and andesitic basalts of the Bol'ba Formation are light gray rocks with a massive structure and porphyritic

and, more seldom, rare porphyritic textures. Plagioclase (or, seldom, clinopyroxene) is a predominant mineral phenocryst. The rock often contains relics of olivine, which is recognized by the kind of its replacement by a secondary mineral (serpentine or iddingsite). The groundmass is almost totally crystalline and consists of plagioclase, pyroxene, and ore mineral microlites. Plagioclase and pyroxene phenocrysts and the groundmass glass are subjected to sericitization, carbonatization, and chloritization.

Plagioclase is the main rock-forming mineral of the andesites, and clinopyroxene is subordinate. Feldspar and the rock groundmass underwent sericitization. The groundmass is composed mostly of plagioclase laths and fine pyroxene and ore mineral crystals.

Dacites are of porphyritic texture; plagioclase is a predominant mineral phenocryst in them. Biotite and tentative-

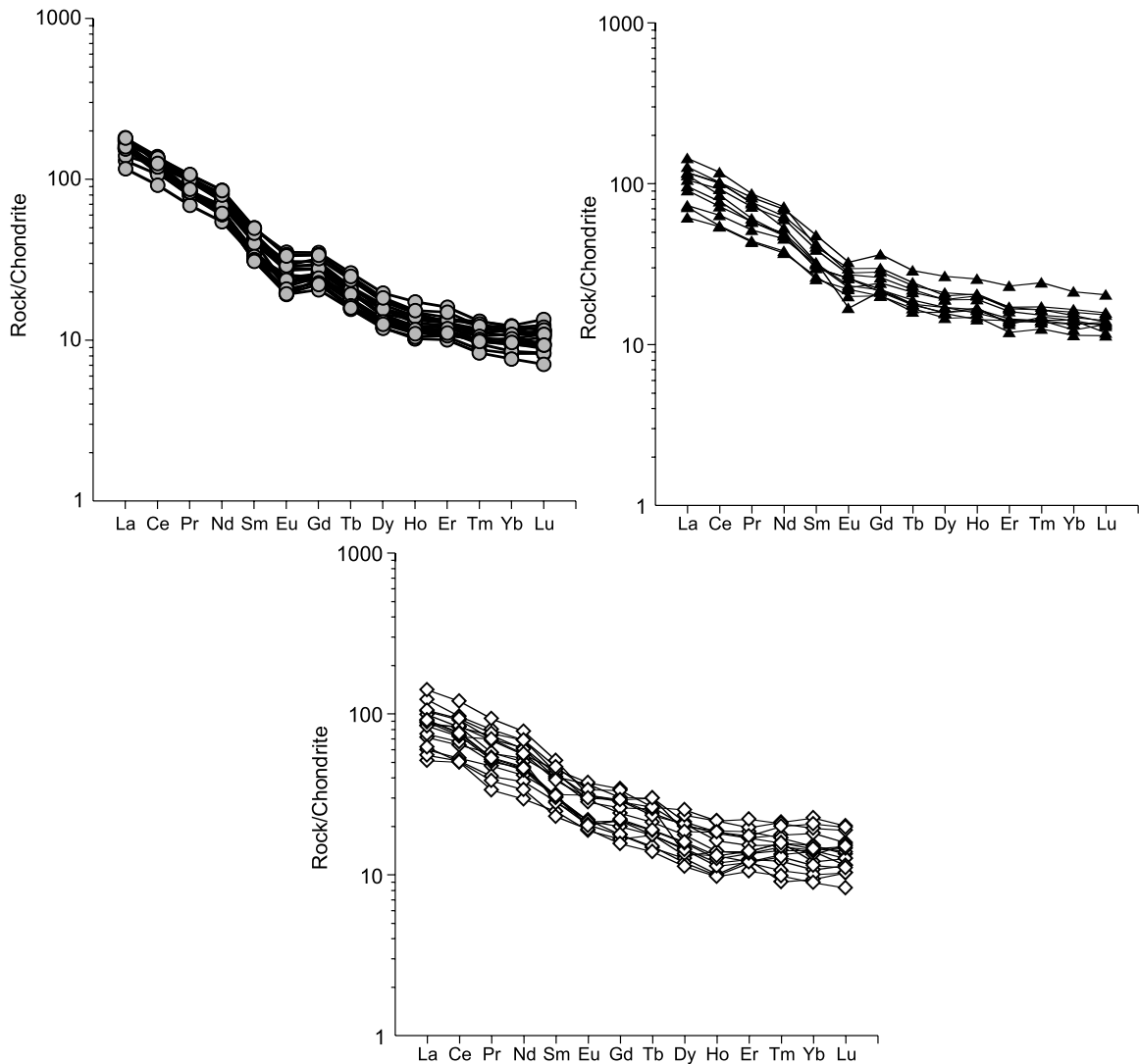


Fig. 6. Chondrite CI-normalized (Sun and McDonough, 1989) REE patterns. Designations follow Fig. 3.

ly altered amphibole are seldom present. Ore mineral is scarce. The groundmass is crystalline and is composed of plagioclase and, seldom, quartz.

Subvolcanic rocks, gabbro, and gabbro-diorites comagmatic with the above volcanics are less subjected to secondary alteration. These are fine- and coarse-grained rocks of plagioclase–two-pyroxene–biotite composition, with a predominance of clinopyroxene. Scarce granodiorites are similar in paragenesis to andesites. Plagioclase is the main rock-forming mineral; clinopyroxene and, sometimes, biotite are subordinate. Some thin sections show the presence of completely replaced amphibole.

### Elemental composition

In  $\text{SiO}_2$  content the volcanics of the Bol'ba Formation vary from basalts to dacites, with a predominance of basaltic

andesites and andesites (Table 2, Fig. 3a). The total content of alkalis varies from 4 to 9 wt.%, which gives grounds to consider all the rocks moderately alkaline (Fig. 3a). This is confirmed by the Zr/Ti–Ni/Y diagram (Fig. 3c).

The behavior of most of the rock-forming elements is well correlated with that of MgO. As the MgO content decreases, the contents of  $\text{SiO}_2$  and  $\text{Na}_2\text{O}$  regularly increase and those of  $\text{TiO}_2$ , CaO, and  $\text{FeO}^*$  decrease in accordance with the crystallochemical properties. No correlation between the contents of  $\text{Al}_2\text{O}_3$  and MgO is observed (Fig. 4).

The contents of compatible trace elements ( $\text{Cr} = 10\text{--}190$  ppm and  $\text{Ni} = 7\text{--}90$  ppm) show a positive correlation with the MgO content. The trends of incompatible elements behave differently. The contents of LILE (Rb, Ba, and Th) increase as the content of MgO decreases. The behavior of Ta is more intricate. Its content varies insignificantly in the case of  $\text{MgO} = 1\text{--}4$  wt.% but drastically drops in the case of

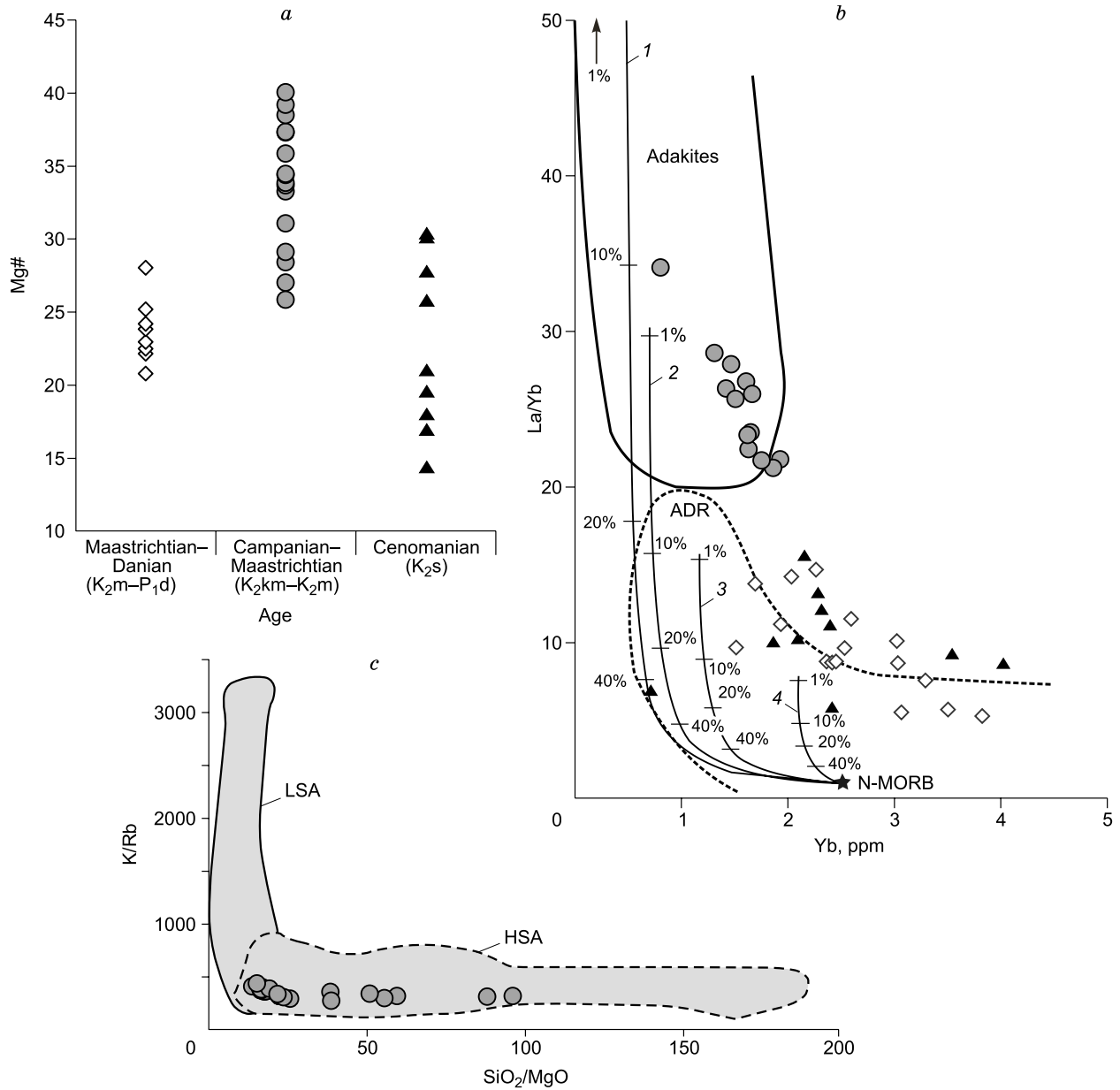


**Fig. 7.** Mg#–age (Mg# = MgO/(MgO + FeO\*)) (a), La/Yb–Yb (after Defant and Drummond (1990), modified) (b), and K/Rb–SiO<sub>2</sub>/MgO (after Martin et al. (2005)) (c) diagrams for volcanics of intermediate composition. ADR field— island-arc andesites, dacites, and rhyolites. Boundaries of the adakite and ADR fields are given after Richards and Kerrich (2007). Trends of partial melting of compositionally different sources: 1, eclogite (garnet:pyroxene = 50:50), 2, 25% garnet amphibolite (25:75), 3, 10% garnet amphibolite (10:90), 4, amphibolite, after Castillo (2012), N-MORB, after Sun and McDonough (1989). Designations follow Fig. 3. LSA, HSA, see the text for explanation.

MgO > 4 wt.%. All studied volcanics show no correlation between the contents of MgO and the contents of HREE and Y.

The N-MORB-normalized trace-element patterns of the studied samples show distinct positive Pb, K, Ba, Rb, and Cs anomalies and a weak negative Ta–Nb anomaly (Fig. 5). Almost all rocks show a negative Eu anomaly. An important feature of the Bol’ba volcanics is stable enrichment in LREE

relative to HREE, as evidenced from their steeply dipping REE patterns (Fig. 6) and high La/Yb ratios (14–34) (Table 2).

The <sup>143</sup>Nd/<sup>144</sup>Nd ratios in the basalts and andesitic basalts of the Bol’ba complex vary over a narrow range of values, 0.51279–0.51281. The ratios of Pb isotopes are as follows: <sup>206</sup>Pb/<sup>204</sup>Pb = 18.63–18.77, <sup>207</sup>Pb/<sup>204</sup>Pb = 15.56–15.60, and <sup>208</sup>Pb/<sup>204</sup>Pb = 38.49–38.62 (Table 2).

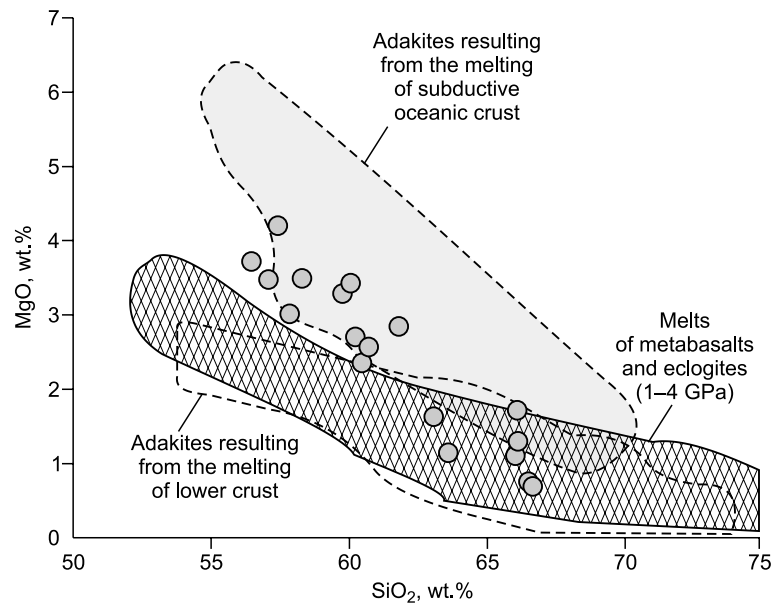


**Fig. 8.** MgO–SiO<sub>2</sub> diagram for the volcanics of the Bol'ba Formation. Fields of the experimental data on melting of metabasalts and eclogites at 1–4 GPa are given after Rapp et al. (1991), Sen and Dunn (1994), Rapp and Watson (1995), Springer and Seek (1997), and Skjerlie and Patiño Douce (2002); fields of adakites melted out of the subducting oceanic crust are given after Defant and Drummond (1993), Kay and Kay (1993), Drummond et al. (1996), Stern and Kilian (1996), Martin (1999), Sajona et al. (2000), and Yogodzinski (2001); and field of adakites melted out of the lower crust is given after Atherton and Petford (1993), Muir et al. (1995), Petford and Atherton (1996), and Johnson et al. (1997). Designations follow Fig. 3.

## DISCUSSION

Elements Na, K, and Ca as well as LILE (Sr, Ba, Rb, Cs, and Pb) are mobile during hydrothermal and metamorphic processes, whereas HFSE and REE, especially HREE, are inert (MacLean, 1990; Jenner, 1996; Hawkesworth et al., 1997). Rare-earth elements and HFSE can be remobilized under interaction of rock with large volumes of hot (>400 °C) fluid solutions saturated with chlorides (Van Dongen et al., 2010). According to microscopic studies, the reference samples of the Bol'ba Formation rocks underwent, to varying degrees, only low-temperature (<300 °C (Miyashiro, 1973)) hydrothermal alterations (carbonatization, chloritization, sericitization, and serpentinization). For this reason, when discussing magma genesis, we will focus the main attention on the behavior of elements inert in the presence of water fluid (HFSE and REE).

### Composition and magma genesis

The volcanics of the Sinancha Formation (K<sub>2</sub>s) and Maastrichtian–Danian andesites (K<sub>2</sub>m–P<sub>1</sub>d) in the south of the ESAVB are considered to be suprasubductional (Simanenko and Khanchuk, 2003; Martynov et al., 2007). The Bol'ba Formation accumulated, most likely, in a different geodynamic setting, because the studied andesite and andesite–dacite samples (SiO<sub>2</sub> = 57–63 wt.%) differ from the suprasubductional volcanics in higher Mg# (MgO/(MgO + FeO\*)) values (Fig. 7a) and LREE enrichment.

Taking into account their high La/Yb ratios, we can classify these rocks as adakites (Fig. 7b). Martin et al. (2005) divided adakites into highly silicic (HSA) and lowly silicic (LSA). Adakites of the Bol'ba Formation tend to HSA by

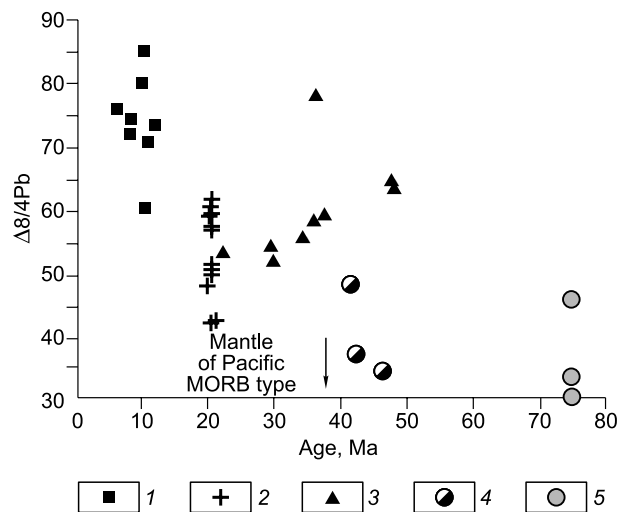


**Fig. 9.**  $\Delta 8/4\text{Pb}$  values in the basalts of different ages of the Sikhote-Alin and Sea of Japan (Chashchin et al., 2011; Martynov et al., 2017) and in the basalts and basaltic andesites of the Bol'ba Formation. 1, Miocene–Pliocene basalts of the eastern Sikhote-Alin; 2, Middle Miocene basalts of the Sea of Japan; 3, Eocene–Oligocene–Early Miocene basalts of the eastern Sikhote-Alin; 4, Early Eocene adakites of the southwestern Sikhote-Alin; 5, volcanics of the Bol'ba Formation.  $\Delta 8/4\text{Pb} = [(^{208}\text{Pb}/^{204}\text{Pb})_{\text{sample}} - (^{208}\text{Pb}/^{204}\text{Pb})_{\text{NHRL}}] \cdot 100$ ;  $(^{208}\text{Pb}/^{204}\text{Pb})_{\text{NHRL}} = 1.209(^{206}\text{Pb}/^{204}\text{Pb})_{\text{sample}} + 15.627$ .

the contents of MgO (<4 wt.%), Sr (<900 ppm), and CaO + Na<sub>2</sub>O (<10 wt.%), falling in the corresponding composition field in the discrimination diagram (Fig. 7c).

Despite numerous studies of adakites, their origin is still debatable. The most common models are as follows: (1) high-pressure fractionation of water-saturated melts, with deposition of garnet and amphibole (Müentener et al., 2001; Prouteau and Scaillet, 2003; Ribeiro et al., 2016); (2) melting of the metamorphosed lower continental crust as a result of its delamination (Atherton and Petford, 1993; Kay and Kay, 1993); (3) partial melting of the eclogitized basalt layer of subducting oceanic plate (Kay, 1978; Defant and Drummond, 1990; Yogodzinski et al., 2001).

The model implying the formation of adakites through the partial melting of the metamorphosed lower continental crust was used for the central segment of the Andes (Goss et al., 2013). The crust there is 65–70 km thick; the adakite lavas have Sm/Yb = 4–9. According to the gravimetric data, the continental crust in the southern Far East is no thicker than 30 km (Petrishchevskii, 1988), and the adakites are characterized by Sm/Yb = 3–4 (Table 2).

In the binary MgO–SiO<sub>2</sub> diagram with the experimental data on melting of compositionally different sources, the figurative points of the Bol’ba Formation adakites form a trend similar to that of oceanic-crust melts (Fig. 8). The highly silicic composition of the studied samples does not contradict this fact and gives grounds to classify them as HSA. Such rocks are usually treated as products of oceanic-crust melting under minimum interaction between the melt and mantle peridotite (Drummond et al., 1996). The same origin of the Bol’ba adakites is confirmed by their  $\Delta 8/4Pb$  values abnormally low for the ESAVB (30–46) (Fig. 9),

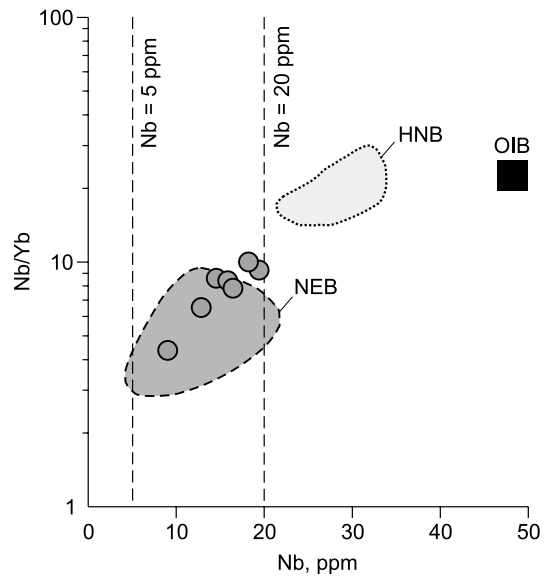


**Fig. 10.** Nb/Yb–Nb diagram for mafic volcanics (54% ≤ SiO<sub>2</sub>). NEB and HNB, after Defant et al. (1992), Kepezhinskas et al. (1997), Aguilon-Robles et al. (2001), Xia et al. (2004), Castillo et al. (2007), Wang (2008), and Macpherson et al. (2010); OIB, after Sun and McDonough (1989). Designations follow Fig. 3.

which suggests the contribution of oceanic basalts with the isotope parameters of the Pacific MORB to magma genesis.

In island-arc systems, e.g., in the Kamchatka region (Perepelov et al., 2013), adakites are often associated with specific high-Nb and Nb-enriched basalts (HNB and NEB, respectively). In the Nb/Yb–Nb diagram (Fig. 10), the compositions of the Bol’ba basalts also fall in the field of these

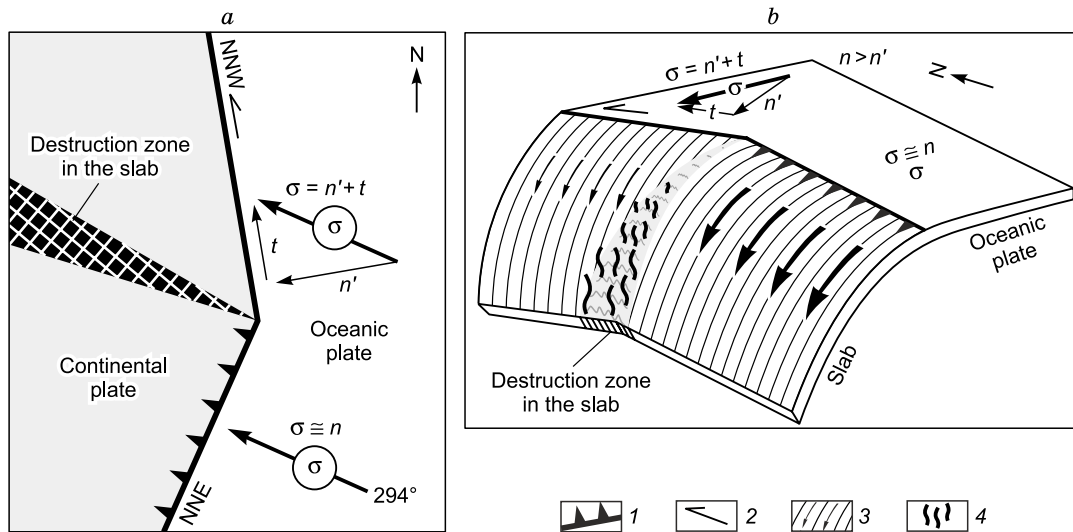


**Fig. 11.** Principal scheme of formation of a breakup zone in subducting slab under orthogonal and oblique interaction between oceanic and continental plates: in plan (a) and in axonometric projection (b).  $\sigma$ , vector of the motion of oceanic plate and its components:  $n$ , normal component coinciding with the vector of the oceanic-plate motion,  $n'$ , normal component under oblique interaction of plates,  $t$ , tangential (shear) component. 1, subduction zone boundary; 2, shearing direction; 3, direction of the subducting-slab motion; 4, penetrating Pacific asthenospheric MORB flow. See the text for explanation.

rocks. This is, most likely, the first finding of igneous NEB–adakite association in the ancient Sikhote-Alin volcanic complexes.

### Geodynamic interpretation

A NEB–adakite association is commonly treated as a result of slab breakup and intrusion of the oceanic asthenosphere into the suprasubductional mantle (Yogodzinski et al., 2001; Levin et al., 2002, 2004; Falloon et al., 2007). With regard to the Pb isotope data, oceanic asthenospheric diapirism within the eastern margin of Eurasia took place probably at the major stage of the opening of the Sea of Japan (~22 Ma, basalts,  $\Delta 8/4\text{Pb} \sim 50$ ) and at the beginning of the breakup of the subducting oceanic lithosphere as a result of shearing (~45 Ma, adakites,  $\Delta 8/4\text{Pb} = 33\text{--}48$ ) (Martynov et al., 2017). The studied adakites of the Bol'ba Formation also have abnormal low (for the ESAVB) contents of radiogenic lead (~74.5 Ma,  $\Delta 8/4\text{Pb} = 30\text{--}46$ ) but formed much earlier, when the southern part of the volcanic belt was at the subduction stage of evolution. Since the general lateral direction of the oceanic-plate motion did not change within 85–74 Ma (Engebretson et al., 1985), the geodynamic regime might have been controlled by regional factors, e.g., the configuration of the continental boundary.

Geodynamic reconstructions (Golozubov, 2006) showed that the zone of convergence of oceanic and continental plates changed its direction from N–NE to N–NW at 48°–49°N in the Late Cretaceous (Fig. 11). Near-orthogonal interaction of two plates ( $\sigma \approx n'$ ) resulted in subduction, and their oblique interaction caused a breaking of the motion vector ( $\sigma$ ) into normal subduction ( $n'$ ) and tangential shearing ( $\tau$ ) components. The latter led to sinistral shears, inevitable breakup of the oceanic plate, increase in the slab permeability, and intrusion of the Pacific asthenospheric mantle into the subcontinental lithosphere. The temperature growth caused melting of the metamorphosed basalts of the oceanic plate and the formation of adakite melts.

### CONCLUSIONS

Based on the geological, petrogeochemical, and isotope studies of the volcanics of the Late Cretaceous Bol'ba Formation in the northern Sikhote-Alin, we have established:

(1) A petro- and geochemical difference between these rocks and the Cenomanian and Maastrichtian–Danian suprasubductional volcanics in the southern sector of the eastern Sikhote-Alin.

(2) Low contents of HREE (Y, Yb, and Lu) and high La/Yb ratios, giving grounds to classify the studied rocks as adakites. The associated basalts are enriched in Nb and are ascribed to NEB.

Since igneous NEB–adakite associations are an indicator of subducting-plate breakup settings and the Sikhote-Alin volcanics have low  $\Delta 8/4\text{Pb}$  values, we have concluded that

the northern sector of the ESAVB evolved in a specific geodynamic regime in the Late Cretaceous, which was governed by the geometry of convergence of continental and oceanic plates.

The effect of local factors, first of all, the configuration of the continental boundary, must be taken into account during the reconstruction of geologic events in the zones of convergence of oceanic and continental plates.

### REFERENCES

- Aguillon-Robles, A., Caimus, T., Bellon, H., Maury, R.C., Cotton, J., Bourgeois, J., Michaud, F., 2001. Late Miocene adakites and Nb-enriched basalts from Vizcaino Peninsula, Mexico: indicators of East Pacific Rise subduction below southern Baja California. *Geology* 29 (6), 531–534.
- Argentov, V.V., Gnibidenko, G.S., Popov, A.A., Potap'ev, S.V., 1976. The Deep Structure of Primorye (from Deep Seismic Sounding Data) [in Russian]. Nauka, Moscow.
- Atherton, M.P., Petford, N., 1993. Generation of sodium-rich magmas from newly underplated basaltic crust. *Nature* 362 (6416), 144–146.
- Bogatikov, O.A., Morozov, A.F., Petrov, O.V., 2009. Petrographic Code of Russia. Igneous, Metamorphic, Metasomatic, and Impact Rocks [in Russian]. VSEGEI, St. Petersburg.
- Budnitskiy, S.Y., Ignatiev, A.V., Velivetskaya, T.A., 2013. Method for measurement of argon isotopes in helium flow for K/Ar geochronology. *Mineral. Mag.* 77 (5), 788.
- Castillo, P.R., 2012. Adakite petrogenesis. *Lithos* 134–135, 304–316.
- Castillo, P.R., Rigby, S.J., Solidum, R.U., 2007. Origin of high field strength element enrichment in volcanic arcs: geochemical evidence from the Sulu Arc, southern Philippines. *Lithos* 97 (3–4), 271–288.
- Chashchin, A.A., Nechaev, V.P., Nechaeva, E.V., Blokhin, M.G., 2011. Discovery of Eocene adakites in Primor'e. *Dokl. Earth Sci.* 438 (2), 744–749.
- Defant, M.J., Drummond, M.S., 1990. Derivation of some modern arc magmas by melting of young subducted lithosphere. *Nature* 347 (6294), 662–665.
- Defant, M.J., Drummond, M.S., 1993. Mount St. Helens: potential example of the partial melting of the subducted lithosphere in a volcanic arc. *Geology* 21 (6), 547–550.
- Defant, M.J., Jackson, T.E., Drummond, M.S., Deboer, J.Z., Bellon, H., Feigenson, M.D., Maury, R.C., Stewart, R.H., 1992. The geochemistry of young volcanism throughout western Panama and southeastern Costa Rica: an overview. *J. Geol. Soc.* 149 (4), 569–579.
- Didenko, A.N., Nosyrev, M.Yu., Shevchenko, B.F., Gil'manova, G.Z., 2017. Thermal structure of Sikhote Alin and adjacent areas based on spectral analysis of the anomalous magnetic field. *Dokl. Earth Sci.* 477 (1), 1368–1372.
- Drummond, M.S., Defant, M.J., Kepezhinskas, P.K., 1996. The petrogenesis of slab derived trondhjemite–tonalite–dacite/adakite magmas, in: *Trans. R. Soc. Edinburgh: Earth Sci.* 87 (1–2), 205–216.
- Engebretson, D., Cox, A., Gordon, R.G., 1985. Relative motions between oceanic and continental plates in the northern Pacific basin. *Spec. Pap. Geol. Soc. Am.* 206, 1–159.
- Falloon, T.J., Danyushevsky, L.V., Ariskin, A., Green, D.H., Ford, C.E., 2007. The application of olivine geothermometry to infer crystallization temperatures of parental liquids: Implications for the temperature of MORB magmas. *Chem. Geol.* 241 (3–4), 207–233.
- Freidin, A.I., Lifshits, Yu.Ya., 1957. Geological Map of the USSR, Scale 1:200,000, Sheet M-54-VII [in Russian]. Gosgeoltekhizdat, Leningrad.
- Golozubov, V.V., 2006. Tectonics of Jurassic and Lower Cretaceous Complexes in the Northwestern Framing of the Pacific [in Russian]. Dal'nauka, Vladivostok.

- Goss, A.R., Kay, S.M., Mpodozis, C., 2013. Andean adakite-like high-Mg andesites on the northern margin of the Chilean–Pampean flat-slab (27–28.5° S) associated with frontal arc migration and fore-arc subduction erosion. *J. Petrol.* 54 (11), 2193–2234.
- Hawkesworth, C.J., Turner, S.P., McDermott, F., Peate, D.W., Van Calsteren, P., 1997. U–Th isotopes in arc magmas: implications for element transfer from the subducted crust. *Science* 276 (5312), 551–555.
- Ignatiev, A.V., Velivetskaya, T.A., Budnitskiy, S.Y., 2009. A continuous flow mass spectrometry technique of argon measurement for K/Ar geochronology. *Rapid Commun. Mass Spectrom.* 23 (16), 2403–2410.
- Izokh, E.P., 1966. Lateral zonation of the Sikhote-Alin structure. *Geologiya i Geofizika* 7 (1), 32–44.
- Jenner, G., 1996. Trace element geochemistry of igneous rocks: geochemical nomenclature and analytical geochemistry, in: Wyman, D. (Ed.), *Trace Element Geochemistry of Volcanic Rocks: Applications for Massive-Sulphide Exploration*. Geological Association of Canada. Short Course Notes, Vol. 12, pp. 51–77.
- Johnson, K., Barnes, C.G., Miller, C.A., 1997. Petrology, geochemistry, and genesis of high-Al tonalite and trondhjemites of the Cornucopia stock, Blue Mountains, Northeastern Oregon. *J. Petrol.* 38 (11), 1585–1611.
- Kay, R.W., 1978. Aleutian magnesian andesites: melts from subducted Pacific Ocean crust. *J. Volcanol. Geotherm. Res.* 4 (1–2), 117–132.
- Kay, R.W., Kay, S.M., 1993. Delamination and delamination magmatism. *Tectonophysics* 219 (1–3), 177–189.
- Kepezhinskas, P., McDermott, F., Defant, M.J., Hochstaedter, A., Drummond, M.S., Hawkesworth, C.J., Koloskov, A., Maury, R.C., Bellon, H., 1997. Trace element and Sr–Nd–Pb isotopic constraints on a three-component model of Kamchatka arc petrogenesis. *Geochim. Cosmochim. Acta* 61 (3), 577–600.
- Khanchuk, A.I., 1993. *Geologic Structure and Evolution of the Continental Framing of the Northwestern Pacific*. ScD Thesis [in Russian]. Moscow.
- Krasnyi, L.I., Peng Yunbiao, 1998. Geological Map of the Amur Region and Adjacent Areas, Scale 1:2,500,000 [in Russian]. VSEGEI, St. Petersburg.
- Kudymov, A.V., Voinova, I.P., Tikhonova, A.I., Didenko, A.N., 2015. Geology, geochemistry, and paleomagnetism of rocks of the Utitsa Formation, North Sikhote Alin. *Russ. J. Pacific Geol.* 9 (5), 323–337.
- Levin, V., Shapiro, N., Park, J., Ritzwoller, M., 2002. Seismic evidence for catastrophic slab loss beneath Kamchatka. *Nature* 418 (15), 763–767.
- Levin, V., Droznin, D., Park, J., Gordeev, E., 2004. Detailed mapping of seismic anisotropy with local shear waves in southeastern Kamchatka. *Geophys. J. Int.* 158 (3), 1009–1023.
- Lishnevskii, E.N., 1969. Principle outlines of the tectonics and deep structure of the USSR's Far East continental area, based on gravimetric data, in: *The Structure and Evolution of the Earth's Crust in the Soviet Far East* [in Russian]. Nauka, Moscow, pp. 21–31.
- MacLean, W.H., 1990. Mass change calculations in altered rock series. *Mineral. Deposita* 25 (1), 44–49.
- Macpherson, C.G., Chiang, K.K., Hall, R., Nowell, G.M., Castillo, P.R., Thirlwall, M.F., 2010. Plio–Pleistocene intra-plate magmatism from the southern Sulu Arc, Semporna peninsula, Sabah, Borneo: implications for high-Nb basalt in subduction zones. *J. Volcanol. Geotherm. Res.* 190 (1–2), 25–38.
- Markevich, P.V., Kononov, V.P., Malinovskii, A.I., Filippov, A.N., 2000. Lower Cretaceous Sikhote-Alin Deposits [in Russian]. Dal'nauka, Vladivostok.
- Martin, H., 1999. Adakitic magmas: modern analogues of Archaean granitoids. *Lithos* 46 (3), 411–429.
- Martin, H., Smithies, R.H., Rapp, R., Moyen, J.F., Champion, D., 2005. An overview of adakite, tonalite–trondhjemite–granodiorite (TTG), and sanukitoid: relationships and some implications for crustal evolution. *Lithos* 79 (1–2), 1–24.
- Martynov, Yu.A., Chashchin, A.A., Simanenkov, V.P., Martynov, A.Yu., 2007. Maestrichtian–Danian andesite series of the eastern Sikhote Alin: mineralogy, geochemistry, and petrogenetic aspects. *Petrology* 15 (3), 275–295.
- Martynov, Yu.A., Khanchuk, A.I., Grebennikov, A.V., Chashchin, A.A., Popov, V.K., 2017. Late Mesozoic and Cenozoic volcanism of the East Sikhote-Alin area (Russian Far East): A new synthesis of geological and petrological data. *Gondwana Res.* 47, 358–371.
- Mel'nikov, N.N., 2005. Errors of the double spiking technique in the isotopic analysis of common lead. *Geochem. Int.* 43 (12), 1228–1234.
- Mikhailov, V.A., 1989. Magmatism of Volcanotectonic Structures in the South of the East Sikhote-Alin Volcanic Belt [in Russian]. DVO RAN, Vladivostok.
- Miyashiro, A., 1973. *Metamorphism and Metamorphic Belts*. Allen & Unwin, London.
- Muir, R.J., Weaver, S.D., Bradshaw, J.D., Eby, G.N., Evans, J.A., 1995. Geochemistry of the Cretaceous Separation Plint Batholith, New Zealand: granitoid magmas formed by melting of mafic lithosphere. *J. Geol. Soc.* 152 (4), 689–701.
- Müntener, O., Kelemen, P.B., Grove, T.L., 2001. The role of H<sub>2</sub>O during crystallization of primitive arc magmas under uppermost mantle conditions and genesis of igneous pyroxenites: an experimental study. *Contrib. Mineral. Petrol.* 141 (6), 643–658.
- Natal'in, B.N., Borukaev, Ch.B., 1991. Mesozoic sutures in the southern Far East. *Geotektonika*, No. 1, 84–97.
- Parfenov, L.M., 1984. Continental Margins and Island Arcs of the Northeast Asia Mesozoids [in Russian]. Nauka, Novosibirsk.
- Perepelov, A.B., Puzankov, M.Yu., Chashchin, A.A., Ivanov, A.V., Palesskii, S.V., Shcherbakov, Yu.D., 2013. NEB-type basaltic volcanism in the Kamchatka island-arc system: origin and paleogeodynamic implications, in: *Proceedings of the Fourth All-Russian Research-to-Practice Conference "Geodynamics and Mineralogy of Northeastern Asia"* [in Russian]. GIN BNTs SO RAN, Ulan-Ude, pp. 282–285.
- Petford, N., Atherton, M., 1996. Na-rich partial melts from newly underplated basaltic crust: the Cordillera Blanca Batholith, Peru. *J. Petrol.* 37 (6), 1491–1521.
- Petrishevskii, A.M., 1988. Statistical Gravity Models of the Far East Lithosphere [in Russian]. Dal'nauka, Vladivostok.
- Proureau, G., Scaillet, B., 2003. Experimental constraints on the origin of the 1991 Pinatubo Dacite. *J. Petrol.* 44 (12), 2203–2241.
- Rapp, R.P., Watson, E.B., 1995. Dehydration melting of metabasalt at 8–32 kbar: implications for continental growth and crust–mantle recycling. *J. Petrol.* 36 (4), 891–932.
- Rapp, R.P., Watson, E.B., Miller, C.F., 1991. Partial melting of amphibolite/eclogite and the origin of Archaean trondhjemites and tonalites. *Precambrian Res.* 51 (1–4), 1–25.
- Ribeiro, J., Maury, R., Grégoire, M., 2016. Are adakites slab melts or high-pressure fractionated mantle melts? *J. Petrol.* 57 (5), 839–862.
- Richards, J., Kerrich, R., 2007. Special paper: Adakite-like rocks: their diverse origins and questionable role in metallogenesis. *Econ. Geol.* 102 (4), 537–576.
- Sajona, F.G., Maury, R.C., Pubellier, M., Leterrier, J., Bellon, H., Cotten, J., 2000. Magmatic source enrichment by slab-derived melts in a young post-collision setting, central Mindanao (Philippines). *Lithos* 54 (3–4), 173–206.
- Savatenkov, V.M., Morozova, I.M., Levsky, L.K., 2004. Behavior of the Sm–Nd, Rb–Sr, K–Ar, and U–Pb isotopic systems during alkaline metasomatism: fenites in the outer-contact zone of an ultramafic–alkaline intrusion. *Geochem. Int.* 42 (10), 899–920.
- Sen, C., Dunn, T., 1994. Dehydration melting of a basaltic composition amphibolite at 1.5 and 2.0 GPa: implications for the origin of adakites. *Contrib. Mineral. Petrol.* 117 (4), 394–409.

- Sidorenko, A.V. (Ed.), 1968. Geology of the USSR [in Russian]. Nedra, Moscow, Vol. 9.
- Simanenko, V.P., 1986. Late Mesozoic volcanic arcs of the eastern Sikhote-Alin and Sakhalin. *Tikhookeanskaya Geologiya*, No. 1, 7–13.
- Simanenko, V.P., 1990. Lower Cretaceous basalt–andesite association of the northern Sikhote-Alin. *Tikhookeanskaya Geologiya*, No. 6, 86–95.
- Simanenko, V.P., Khanchuk, A.I., 2003. Cenomanian volcanism of the eastern Sikhote-Alin volcanic belt: geochemical features. *Geochem. Int.* 41 (8), 787–798.
- Skjerlie, K.P., Patiño Douce, A.E., 2002. The fluid-absent partial melting of a zoisite-bearing quartz eclogite from 1.0 to 3.2 GPa: implications for melting in thickened continental crust and for subduction-zone processes. *J. Petrol.* 43 (2), 291–314.
- Springer, W., Seek, H.A., 1997. Partial fusion of basic granulites at 5 to 15 kbar: implications for the origin of TTG magmas. *Contrib. Mineral. Petrol.* 127 (1–2), 30–45.
- Steiger, R.H., Jäger, E., 1977. Subcommittee on Geochronology: Convention on the use of decay constants in geo- and cosmology. *Earth Planet. Sci. Lett.* 36 (3), 359–361.
- Stern, C.R., Kilian, R., 1996. Role of the subducted slab, mantle wedge and continental crust in the generation of adakites from the Andean Austral Volcanic Zone. *Contrib. Mineral. Petrol.* 123 (3), 263–281.
- Sukhov, V.I., 1967. Geologic positions, structure, and metallogeny of Late Cretaceous and Cenozoic effusive–extrusive complexes in the Lower Amur region. *Sovetskaya Geologiya*, No. 4, 45–56.
- Sun, S.S., McDonough, W.F., 1989. Chemical and isotopic systematics of oceanic basalts: implications for mantle composition and processes, in: Saunders, A.D., Norry, M.J. (Eds.), *Magmatism in the Ocean Basins*. Geological Society Special Publication, London, pp. 313–345.
- Van Dongen, M., Weinberg, R.F., Tomkins, A.G., 2010. REE–Y, Ti, and P remobilization in magmatic rocks by hydrothermal alteration during Cu–Au deposit formation. *Econ. Geol.* 105 (4), 763–776.
- Wang, Q., Wyman, D.A., Xu, J.F., Wan, Y.S., Li, C.F., Zi, F., Jiang, Z.Q., Qiu, H.N., Chu, Z.Y., Zhao, Z.H., Dong, Y.H., 2008. Triassic Nb-enriched basalts, magnesian andesites, and adakites of the Qiangtang terrane (Central Tibet): evidence for metasomatism by slab-derived melts in the mantle wedge. *Contrib. Mineral. Petrol.* 155 (4), 473–490.
- Winchester, J., Floyd, P., 1977. Geochemical discrimination of different magma series and their differentiation products using immobile elements. *Chem. Geol.* 20, 325–343.
- Xia, L.Q., Xu, X.Y., Xia, Z.C., Li, X.M., Ma, Z.P., Wang, L.S., 2004. Petrogenesis of Carboniferous rift-related volcanic rocks in the Tianshan, northwestern China. *Geol. Soc. Am. Bull.* 116 (3), 419–433.
- Yogodzinski, G.M., Lees, J.M., Churlkova, T.G., Dorondor, F., Wonerer, G., Volynets, N., 2001. Geochemical evidence for the melting of subducting oceanic lithosphere at plate edges. *Nature* 409 (6819), 500–504.
- Zonenshain, L.P., Kuz'min, N.I., Natanov, L.M., 1990. Plate Tectonics of the USSR Territory [in Russian]. Nedra, Moscow, Vol. 2.

*Editorial responsibility:* E.V. Sklyarov